Journal Pre-proof

Comparison of Electrodiagnosis, Neurosonography and MR Neurography in localization of Ulnar Neuropathy at the Elbow

Michael J. Ho, Ulrike Held, Klaus Steigmiller, Andrei Manoliu, Andreas Schiller, Ricarda Hinzpeter, Christian Lanz, Carlo Martinoli, Hans H. Jung, Jens A. Petersen

PII: S0150-9861(21)00109-7

DOI: https://doi.org/10.1016/j.neurad.2021.05.004

Reference: NEURAD 997

To appear in: *Journal of Neuroradiology*

Please cite this article as: Ho MJ, Held U, Steigmiller K, Manoliu A, Schiller A, Hinzpeter R, Lanz C, Martinoli C, Jung HH, Petersen JA, Comparison of Electrodiagnosis, Neurosonography and MR Neurography in localization of Ulnar Neuropathy at the Elbow, *Journal of Neuroradiology* (2021), doi: https://doi.org/10.1016/j.neurad.2021.05.004

Comparison of Electrodiagnosis, Neurosonography and MR Neurography in localization of Ulnar Neuropathy at the Elbow

Michael J. Ho, MD[1,2*]; Ulrike Held, PhD[3], Klaus Steigmiller[3], Andrei Manoliu, MD, PhD[4]; Andreas Schiller, MD[5]; Ricarda Hinzpeter, MD[6]; Christian Lanz, MD[7]; Carlo Martinoli, MD[8,9]; Hans H. Jung, MD[10], Jens A. Petersen MD[10]

[1] Department of Diagnostic, Interventional and Pediatric Radiology (DIPR), Inselspital, Bern University Hospital, University of Bern, Switzerland

[2] Department of Neuroradiology, University Hospital Bonn, Bonn, Germany.

[3] Epidemiology, Biostatistics and Prevention Institute, Department of Biostatistics, University of Zurich, Zurich, Switzerland

[4] Department of Psychiatry, Psychotherapy and Psychosomatics, Psychiatric Hospital, University of Zurich, Zurich, Switzerland

[5] Division of Plastic Surgery and Hand Surgery, University Hospital Zurich, Zurich, Switzerland

[6] Institute of Diagnostic and Interventional Radiology, University Hospital Zurich, University of Zurich, Zurich, Switzerland

[7] Department of Neurology, Schulthess Klinik, Zurich, Switzerland

[8] Department of Health Sciences (DISSAL), Università di Genova - Genova, Italy

[9] IRCCS Ospedale Policlinico San Martino - Genova, Italy

[10] Department of Neurology, University Hospital Zurich and University of Zurich, Zurich, Switzerland

[*]Corresponding author:

Dr. med. Michael J. Ho

Lindenstrasse 41

8008 Zurich

Switzerland

mikeho@hotmail.de

Highlights

1) MR Neurography with T2 CNR showed better results compared to the other diagnostic tests in precise localization of UNE.

2) Differences for all diagnostics tests between affected arms of patients and healthy control arms were most frequently the largest at measure intervals D2 to P0 or P0 to P2.

3) Additional imaging with MRN DTI is a promising technique that could be used as a non-invasive biomarker for localization of UNE.

Introduction: In patients with ulnar neuropathy at the elbow (UNE) the precise determination of the site of lesion is important for subsequent differential diagnostic considerations and therapeutic management. Due to a paucity of comparable data, to better define the role of different diagnostic tests, we performed the first prospective study comparing the diagnostic accuracy of short segment nerve stimulation, nerve ultrasonography, MR neurography (MRN), and diffusion tensor imaging (DTI) in patients with UNE.

Methods: UNE was clinically diagnosed in 17 patients with 18 affected elbows. For all 18 affected elbows in patients and 20 elbows in 10 healthy volunteers, measurements of all different diagnostic tests were performed at six anatomical positions across the elbow with measuring points from distal (D4) to proximal (P6) in relation to the medial epicondyle (P0). Additional qualitative assessment regarding structural changes of surrounding nerve anatomy was conducted.

Results: The difference between affected arms of patients and healthy control arms were most frequently the largest at measure intervals D2 to P0 and P0 to P2 for electrophysiological testing, or measure points P0 and P2 for all other devices,

respectively. At both levels P0 and at P2, T2 contrast-to-noise ratio (CNR) of MRN and mean diffusivity (MD) of DTI-based MRN showed best accuracies.

Discussion: This study revealed differences in diagnostic performance of tests concerning a specific location of UNE, with better results for T2 contrast to noise ratio (CNR) in MRN and mean diffusivity of DTI-based MRN. Additional testing with MRN and nerve ultrasonography is recommended to uncover anatomical changes.

Keywords: MR Neurography, ulnar nerve, nerve ultrasound, DTI, ulnar neuropathy, elbow

Introduction

Ulnar neuropathy at the elbow (UNE) is the second-most common entrapment neuropathy after carpal tunnel syndrome. In patients with UNE two mechanisms are causing the majority of cases: compression in the retroepicondylar groove (RTC) and entrapment by the humeroulnar aponeurotic arcade (HUA), which connects the two heads of the flexor carpi ulnaris. The HUA is located about 2 cm distal to the medial epicondyle. While conventional electrodiagnostic testing can detect UNE, the precise localization of the site of compression is more challenging. Regularly, the clinical diagnosis of UNE is confirmed using a 10-cm nerve conduction study (NCS), an electrodiagnostical (EDx) technique with high specificity and much lower sensitivity that has varied across studies from 37% to 86%.[1] A short-segment NCS (SSNCS, "inching") is an EDx approach with a higher diagnostic accuracy.[2-5]

In the last two decades, progress has been made in peripheral nerve imaging. The ulnar nerve can be now depicted with excellent resolution using advanced ultrasound (US) technology, which has been recommended as a reliable additional test in the diagnosis of UNE.[6-7] Neuromuscular ultrasound highlights underlying causes of ulnar neuropathy, such as

structural abnormalities, ganglia, or osteophytes.[8] However, US studies measuring ulnar nerve thickness in UNE patients have reported a highly variable sensitivity of 46% to 100% and specificity of 43% to 97%.[9-16] In one study, the diagnostic accuracy of US (77%) was lower than that of SSNCSs (85%) and 10-cm NCSs (83%).[17] To precisely localize UNE, SSNCSs and US may be used complementarily.[7]

Magnetic resonance (MR) neurography helps improve localization and diagnostic accuracy for a variety of peripheral neuropathies[18-21], including UNE (22). A T2 signal intensity increase due to intraneural edema may be of diagnostic value [18]: A hyperintense T2-weighted signal has been reported in up to 60% of asymptomatic healthy individuals[23], however, the quantification of ulnar nerve T2-weighted signal hyperintensities at 3 Tesla offers a sensitivity of 83% in the detection of UNE.[24] Nerve caliber enlargement differentiates severe from mild UNE.[24]

Diffusion tensor imaging-based MR neurography (DTI), which measures the movement of water molecules along the course nerve with fractional anisotropy (FA) and radial to the course of the nerve with mean diffusivity (MD), has been proposed as a surrogate marker for nerve integrity.[26, 27] A recent study suggests that DTI is a very sensitive and specific technique for assessing UNE.[25]

Due to a paucity of comparative data, to better define the role of different diagnostic tests, we performed a prospective study comparing the diagnostic accuracy of SSCNS, nerve ultrasound, MR neurography, and DTI-based MR-neurography in patients with a diagnosis of UNE established by clinical examination. In patients with UNE, we examined the additional diagnostic value of tests regarding their ability to establish a differential diagnosis.

Materials and Methods

Participants, history and clinical examination

The study was approved by the local ethics committee (KEK-ZH-No. 2013-0291), and informed consent was obtained from all subjects in writing prior to the investigation. All tests and postprocessings were performed between May 2016 and February 2019. Patients with suspected UNE were recruited, a patient history was taken, and demographic and clinical data were collected by an experienced neurologist (J.P.). During a clinical examination, hand muscle wasting, hand muscle weakness as rated by the Modified Research Council (MRC) Rating Scale and light touch / pinprick sensation in the hand were recorded[29]. Inclusion criteria for UNE patients were at least one of the following presenting symptoms typical for UNE: (1) numbness or paresthesia of the fifth digit and the ulnar side of the fourth digit of the hand and / or in the dorsal cutaneous branch; (2) weakness or clumsiness of the muscles innervated by the ulnar nerve; (3) medial elbow pain radiating to the forearm or hand.[7, 28] Exclusion criteria for patients and control subjects were alternate or confounding diagnoses such as polyneuropathy and any condition causing polyneuropathy (e.g., diabetes), hereditary neuropathy with liability to pressure palsies, multifocal motor neuropathy with conduction block (MMN), or motor neuron disorders (e.g., monomelic amyotrophy, amyotrophic lateral sclerosis – ALS).[7] Further exclusion criteria for control subjects included (1) sensory symptoms of the fourth and fifth digits and the ulnar side of the fourth digit of the hand and / or in the dorsal cutaneous branch; (2) ulnar nerve muscle weakness; (3) a history of elbow surgery or trauma; (4) clinical signs and symptoms of ulnar nerve abnormalities. FIGURE 1 illustrates the study design with analogy of the measurements of different diagnostic tests in correlation to the anatomical positions 6 cm proximal (P6) to 4 cm distal (D4) of the medial epicondyle of the olecranon (P0).

FIGURE 1

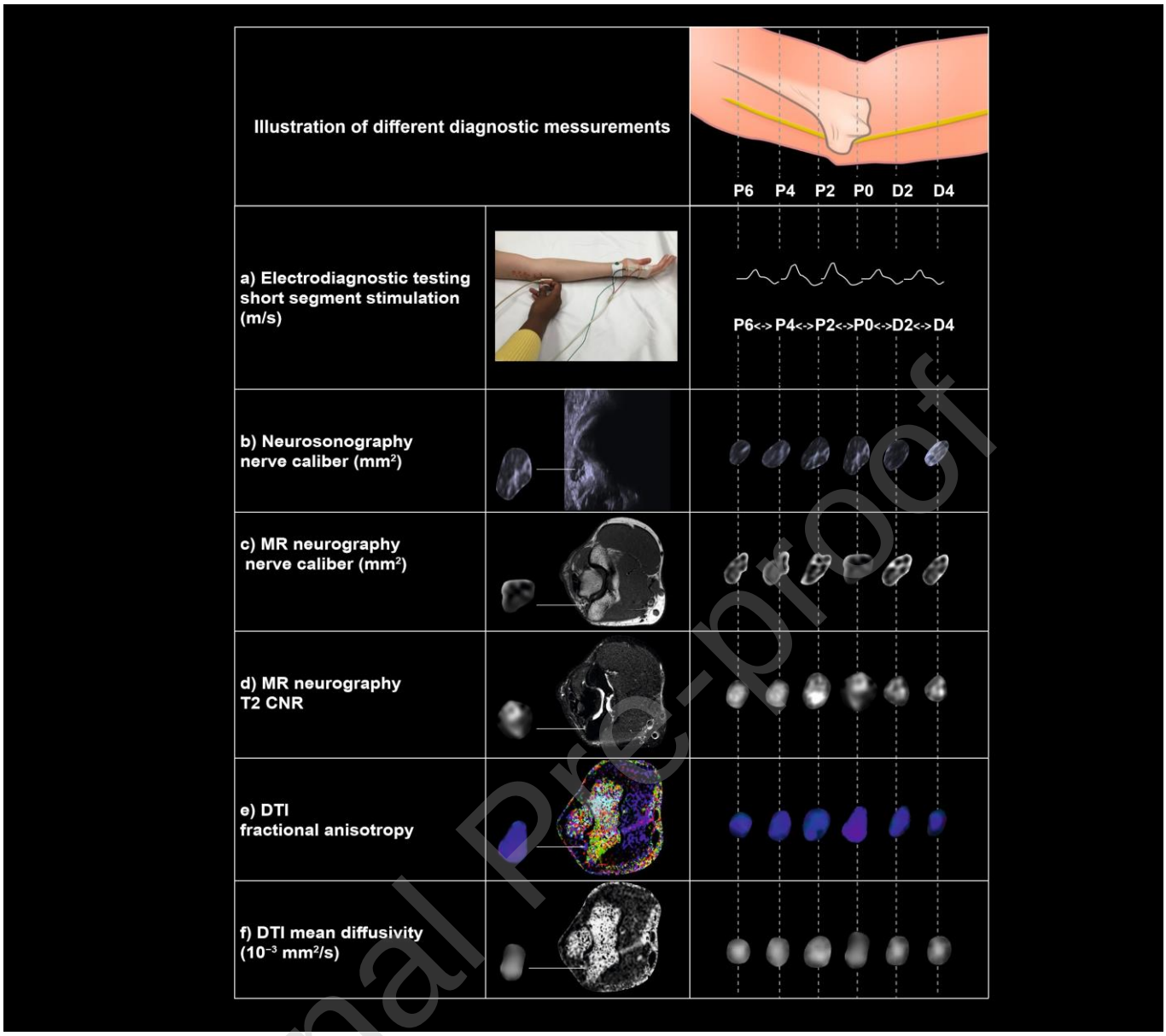

FIGURE 1 illustrates different diagnostic measurements: a) electrodiagnostical testing with short-segment (2cm) NCS (SSNCS)- "inching" (m/s), b) neurosonography nerve caliber (mm^2), c) MR neurography nerve caliber (mm^2), d) MR neurography T2 contrast to noise ratio (CNR) e) DTI fractional anisotropy, f) and mean diffusivity (10^{-3} mm^2/s) with respect to the measuring points D4 to P6 in relation to the medial epicondyle (P0).

Electrodiagnosis (EDx)

A neurologist (J.P.) performed standardized ulnar NCSs on each subject's elbows, using a standard EMG system (Nicolet Viking, Natus Medical Incorporated, San Carlos, USA) for all patients. Elbow position was moderate flexion between 70º to 90º.

For SSCNs, markers were placed at the medial epicondyle (P0); 2 and 4cm distal (D2, D4); and 2, 4, and 6cm proximal (P2, P4, and P6) along the course of the ulnar nerve.[5, 30] Supramaximal stimulation (stimulus duration 0.2 ms) was conducted with the cathode placed 8cm proximal to the Abductor digiti minimi (ADM) muscle and at each of the markers across the elbow. Compound muscle action potentials (CMAPs) were recorded from the ADM muscle using surface electrodes. Latencies (in milliseconds) were measured from the stimulus to the onset of the CMAP and amplitudes (in millivolts) from the negative peak to the baseline.

Ultrasonography

For US studies, patients were lying supine with the elbow in the same position as it was for the EDx studies. All sonographic examinations of the elbow were conducted by either a musculoskeletal radiologist or a neurologist with experience in musculoskeletal sonography. The ulnar nerve cross-sectional area (CSA) was measured across both elbows at each marker (D2, D4, P0, P2, P4, P6)[7, 14], at the wrist, and at the mid-point of the upper arm using an US device (SIEMENS Acuson x700, Simenes Healthcare, Erlangen, Germany) - with an 18 MHz linear array transducer. Minimal pressure was applied to the transducer to avoid extrinsic nerve compression. The transducer was held perpendicular to the skin with minor angle adjustments performed to ensure that the transducer was perpendicular to the nerve. In addition, dynamic sonography was performed by flexing the elbow, whereby the transducer

remained in situ relative to the level of the medial epicondyle Images were saved in TIFF format without side, subject, or group labelling.

MR neurography with DTI

Both elbows of subjects were scanned in a high-field clinical 3T scanner (MAGNETOM Skyra, Siemens Healthcare, Erlangen, Germany). Subjects were in a prone position with one arm overhead. A 4-channel flexible coil (Siemens Healthcare) was placed around the elbow, with the palpable eminence of the ulnar epicondyle centered in the coil. All sequences were transversally oriented. First, the following pulse sequences were performed:

High-resolution T2-weighted fat-suppressed sequence repetition time/echo time 5,800/40 milliseconds, high spectral fat saturation, effective resolution 1.2 x 1.2 x 2.0 mm, field of view 140 × 140 mm, acquisition time 5:18 minutes.

T1 FSE repetition time/echo time 600/18 milliseconds, effective resolution 1.2 x 1.2 x 2.0 mm, field of view 140 × 140 mm, acquisition time 4:26 minutes.

Next, DTI was performed using a conventional ss-EPI sequence: repetition time/echo time 4,400/77 milliseconds, effective resolution 1.2 x 1.2 x 2.0 mm, field of view 140 × 140 mm, b-values of 0 and 1000 s/mm^2, 20 gradient directions, acquisition time 6:12 minutes.

Quantitative image analysis

Two investigators (M.H. and A.M.) used a Siemens Syngo Workstation (Version VB10A, Siemens Healthcare, Erlangen, Germany) to perform quantitative image analysis, measured values were then averaged. Both investigators were blinded to all participant data.

For neurosonography and all images of MRN including DTI, both readers independently placed regions of interest (ROIs) outlining the exact ulnar nerve circumference as previously demonstrated by Keen et al.[31] on the respective sequence images in the ulnar nerve at the

medial epicondyle (P0); 2 and 4 cm distal (D2, D4); and 2, 4, and 6 cm proximal (P2, P4, and P6).

T2 CNR: Ulnar nerve T2 signal intensity was calculated for each section position by measuring signal intensity within the ROI of the nerve (iROI), the signal intensity of an adjacent non-denervated muscle (mROI), and the standard deviation of a measurement of ROI placed in air (SDair) according to the following equation: T2 CNR = $\frac{i(ROI)-m(ROI)}{SDair}$.[24]

CSA in neurosonography: For CSA measurements in neurosonography, manually precise traces of the circumference of the ulnar nerve were drawn for each section position from P6 to D4.

CSA in MRN: Analogous to the measurements of CSA measurements in ultrasonography, manually precise traces of the circumference of the ulnar nerve were drawn for each section position in T1 FSE images.

DTI parameters: For the DTI sequences, parametrical voxel-wise maps of the FA and mean diffusivity MD were automatically generated by the scanner's console. For FA and MD measurements, ROIs for each section position were placed on the respective maps in the ulnar nerve.

Qualitative image assessment

Two raters (M.H. and A.M.) performed qualitative image assessment in consensus regarding structural changes of surrounding nerve anatomy. Neurosonography images and MRN images (high-resolution T2 weighted fat-suppressed sequence and T1 weighted FSE sequence) were investigated with regards to changes in the surrounding structures to the nerve. These included (1) the presence of an epitrochlear anconeus muscle, (2) hypertrophied medial head of the triceps muscle (if exerting more than 50% of the surface of the ulnar groove), (3) bony anomalies, (4) osteophytes, (5) cysts, or (6) ganglia. Dynamic neurosonography examination

and MRN were used to determine whether there was a displacement of the nerve at the level of the ulnar groove.

Statistical methods

Descriptive statistics included mean and standard deviation for the six different measurement devices at measure points P0 and P2, except for electrophysiological testing, where these measure intervals were D2 to P0 and P0 to P2. We have focused on these intervals and measure points when discrimination between affected arms and healthy controls was addressed since the difference between affected arms of patients and healthy control arms were most frequently the largest at measure intervals D2 to P0 and P0 to P2 for electrophysiological testing, or measure points P0 and P2 for all other devices. These statistics are reported separately for affected and unaffected arms of patients, as well as for healthy controls, a group wise comparison was done via ANOVA. For each device, separate graphs illustrate mean ± standard error of the mean (SEM) over all measure points, separately for affected and unaffected arms of patients, as well as for healthy controls. Discrimination between affected arms of patients and healthy controls (both arms) was addressed with ROC analysis. For each device, the measurements at measure points P0 and P2 were used separately to fit smoothed ROC curves to the binary outcome (1=affected arm, 0=healthy control arm). The area under the smoothed ROC curve (AUC) including 95% confidence intervals was compared between devices. All statistical analyses and plots were conducted with the programming language R (R Core Team 2017).[33]

Results

Seventeen patients and 10 healthy control persons with 20 healthy elbows were included in this study. Of the patients, 12 were of female gender. In the 17 patients 18 affected elbows and 16 unaffected elbows were examined. In the female patients age (mean ± standard deviation [SD]) was 47.9 ± 15.4 years. In the male patients age (mean ± SD) was 40.3 ± 18.8 years. In the healthy controls, 20 elbows were examined. Five healthy controls were women (mean age 33 years; SD ± 7.9 years) and five men (mean age 31.2 years; SD ± 4.1 years). The control group was not age-or sex-matched. Even though there were discrepancies between tests with respect to the extent of measurements – the difference between affected arms of patients and healthy control arms were most frequently the largest at measure intervals D2 to P0 and P0 to P2 for electrophysiological testing, or measure points P0 and P2 for all other devices, respectively - as shown in FIGURE 2. All descriptive statistics for these measure points can be found in TABLE 1.

FIGURE 2

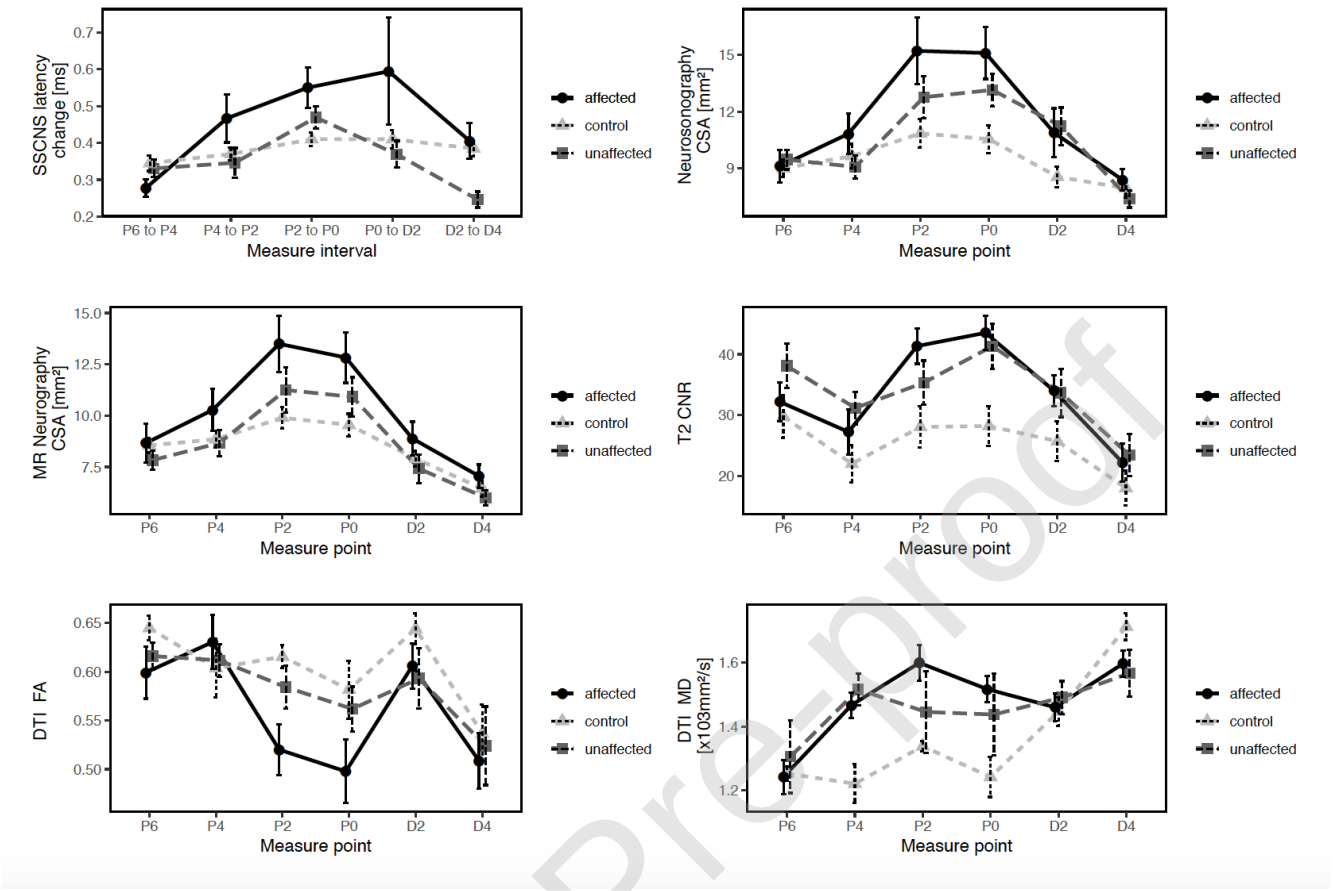

FIGURE 2 depicts ulnar nerve SSNCS CMAP latency changes (ms), summarized as mean ± 1 standard error across all intervals from P6 to D4. For all other measurement devices, six measurement points from P6 to D4 are depicted. For all six measurement devices, these graphs are reported separately for affected and unaffected arms of patients, as well as for healthy controls.

TABLE 1

	Measure point / interval	Affected n=18	Unaffected n=16	Healthy controls n=20	p-value
Electrophysiological testing, mean (sd)	P0 to D2	0.6 (0.6)	0.4 (0.1)	0.4 (0.1)	0.198
Neurosonography CSA [mm^2], mean (sd)	P0	15.1 (5.8)	13.2 (3.1)	10.6 (3.3)	0.008
MR Neurography CSA [mm^2], mean (sd)	P0	12.8 (5.2)	10.9 (3.3)	9.6 (2.4)	0.04
T2 CNR, mean (sd)	P0	43.5 (11.7)	41.3 (12.9)	28.2 (14.7)	0.002
DTI FA [unitless], mean (sd)	P0	0.5 (0.1)	0.6 (0.1)	0.6 (0.1)	0.114
DTI MD (x103mm^2/sec), mean (sd)	P0	1.5 (0.2)	1.4 (0.4)	1.2 (0.3)	0.019
Electrophysiological testing, mean (sd)	P2 to P0	0.6 (0.2)	0.5 (0.1)	0.4 (0.1)	0.032
Neurosonography CSA [mm^2], mean (sd)	P2	15.2 (7.4)	12.8 (4.0)	10.8 (3.4)	0.049
MR Neurography CSA [mm^2], mean (sd)	P2	13.5 (5.9)	11.2 (3.8)	9.9 (2.4)	0.041
T2 CNR, mean (sd)	P2	41.4 (12.0)	35.3 (12.6)	28.1 (15.3)	0.017
DTI FA [unitless], mean (sd)	P2	0.5 (0.1)	0.6 (0.1)	0.6 (0.1)	0.004
DTI MD (x103mm^2/sec), mean (sd)	P2	1.6 (0.2)	1.4 (0.4)	1.3 (0.1)	0.014

TABLE 1. Mean and standard deviations of the measurement devices at P0 and P2, separated into affected and unaffected arms of patients, as well as healthy controls.

As ROC analysis [FIGURE 3 & 4] shows that diagnostic performance was similar for electrodiagnostical testing for the interval P2 - P0 (AUC = 0.77, 95% confidence interval (CI): 0.58 - 0.96), CSA in neurosonography in P0/P2 (AUC = 0.79, 95% CI: 0.64 - 0.93/AUC = 0.73, 95% CI: 0.57 - 0.90), CSA in MRN in P0/P2 (AUC = 0.72, 95% CI: 0.55 - 0.90/AUC = 0.75, 95% CI: 0.65 - 0.91) and FA of DTI in P0/P2 (AUC = 0.73, 95% CI: 0.55 - 0.91/ AUC = 0.76, 95% CI: 0.59 - 0.94). At the interval from D2 to P0, diagnostic performance of electrodiagnostical testing (AUC = 0.57, 95% CI: 0.36 - 0.78) was inferior to other tests. At both levels P0 and at P2, T2 CNR of MRN (AUC = 0.8, 95% CI: 0.64 - 0.96/ AUC = 0.82, 95% CI: 0.67 - 0.97) and MD of DTI-based MRN (AUC = 0.86, 95% CI: 0.72 - 1/ AUC = 0.85, 95% CI: 0.69 - 1) performed slightly better.

FIGURE 3

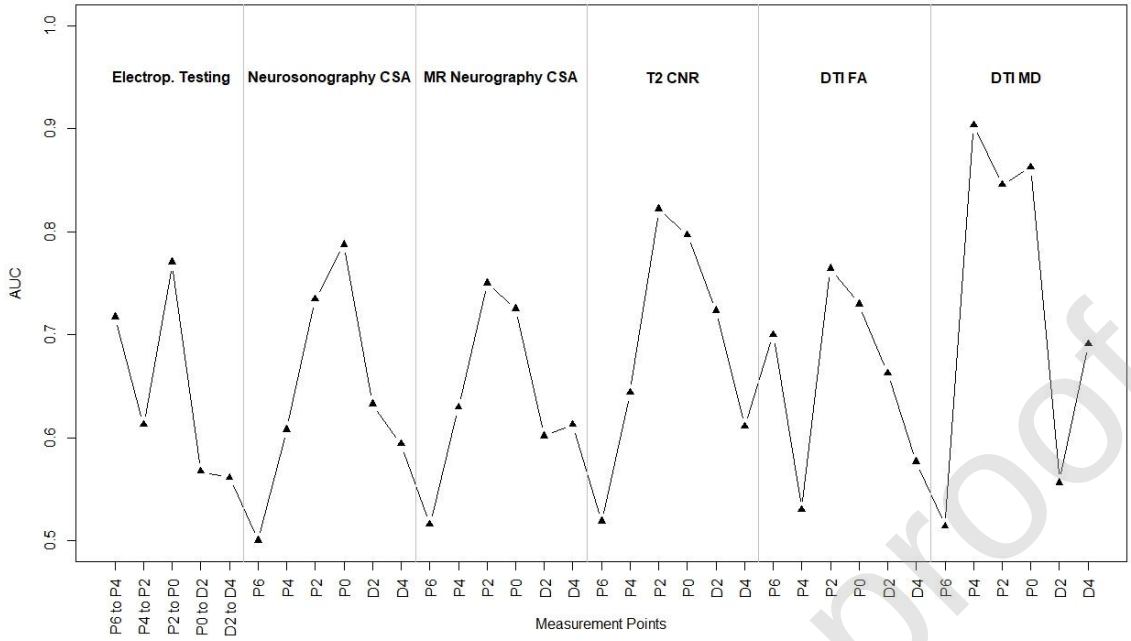

FIGURE 3 depicts the AUC across all measurement points/intervals and devices. For electrophysiological testing, the highest AUC was observed for the intervals P0 to P2 (0.77) and P4 to P6 (0.71). For DTI-MD, the highest AUC was observed for P4 (0.90). For all other devices, measurement at either P0 or P2 resulted in the highest AUC values.

FIGURE 4

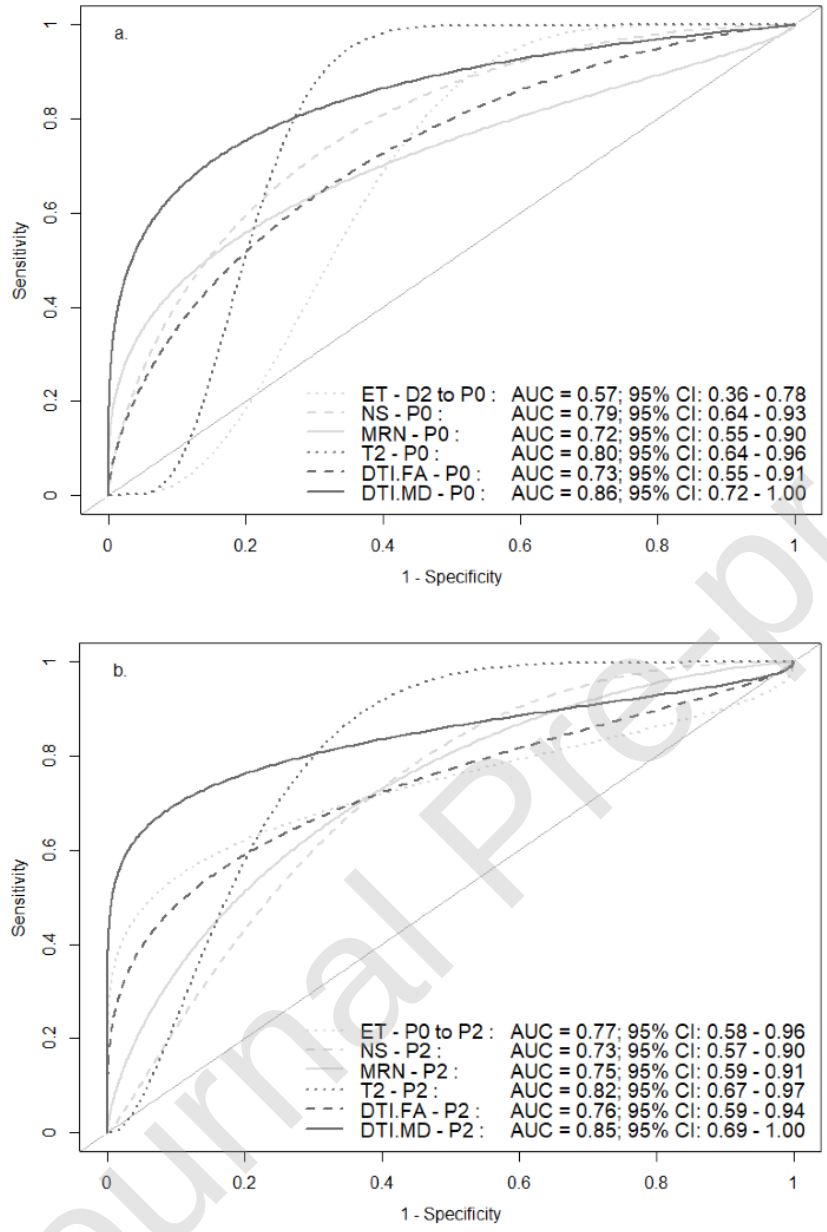

FIGURE 4 depicts the smoothed ROC curves for each device. Panel (a) is based on measurements at measure point P0 and measure interval D2 to P0 for electrophysiological measurement. Panel (b) is based on P2 and P0 to P2 respectively. Each of the ROC curves also includes information on the estimated areas under the curve, with 95% confidence

intervals. There are large discrepancies between the devices: DTI MD demonstrates the most favorable discriminative ability, whereas electrophysiological testing and neurosonography CSA demonstrate the least favorable AUC.

Qualitative image analysis

Dislocation of the nerve during elbow flexion was noted in three of the affected elbows in neurosonography. In one of these cases, a subluxation was also observed in MRN. Bone abnormalities (osteophytes) were seen in two cases in MRN [FIGURE 5 b)] and surrounding soft tissue changes (edema) were seen in two cases in neurosonography and MRN (in MRN in one case corresponding with subluxation of the ulnar nerve). A small cyst originating from the medial aspect of the ulnohumeral joint was seen in MRN in one case. An additional anconeus epitrochlearis muscle was found in one affected elbow in neurosonography and in MRN [FIGURE 5 a)].

FIGURE 5

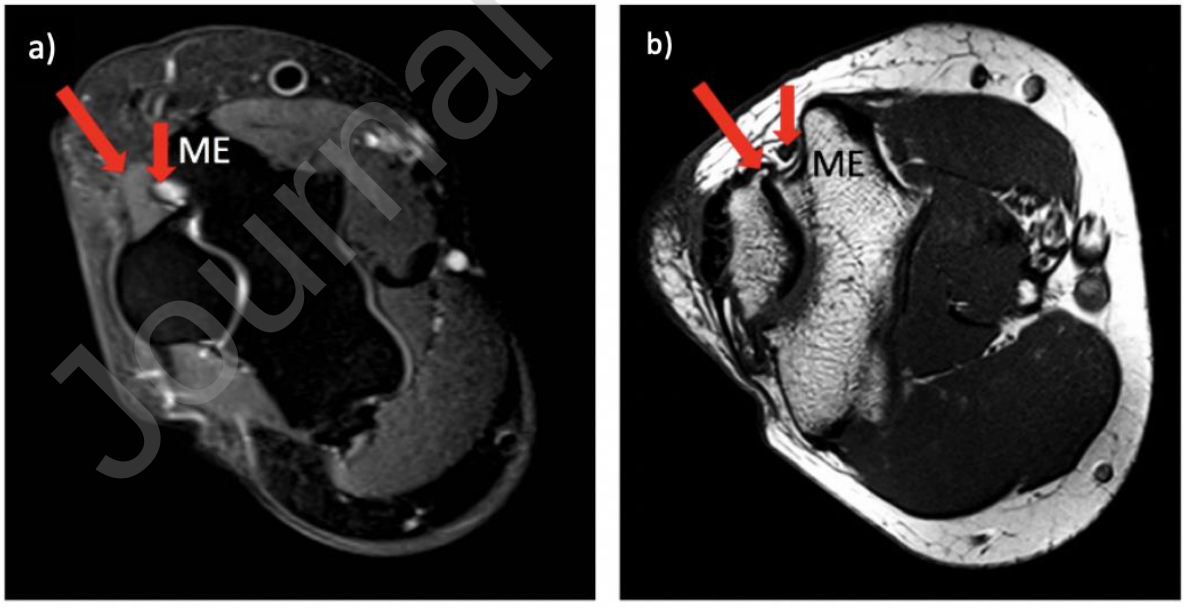

FIGURE 5 shows example findings of MRN: a) additional anconeus epitrochlearis muscle (long arrow) compressing the ulnar nerve (short arrow) which shows a high T2 signal, b)

MRN: osteophyte (long arrow) originating from the medial aspect of the olecranon adjacent to the ulnar nerve (short arrow).

Discussion

Summary of results:

The quantitative results reveal differences in the maximum expression of the measured values with respect to an anatomic position for different tests. Such discrepancies in the precise localization of UNE between findings of different tests have been noted before.[34]

There may be several technical reasons for this. On the one hand, measurements from different tests on the same subject may vary as the subject's position may change, despite utmost care during examination, post-processing, and evaluation. For example, for CSA, a value obtained in MR neurography and sonography in the same unit (mm^2), there are differences at all levels from P6 to D4. In addition, redetermination of the positions in the different tests may have resulted in measurement inaccuracies with respect to the exact postions (P6-D2) in the comparison of the modalities. Furthermore, during an MRI scan, small movements take place, so minor displacements cannot be excluded – even between different MR sequences. In addition, voxel volume and shape of the voxel are important. The commonly preferred anisotropic voxel geometry allows a high in-plane resolution, but could on the other side affect the delineation of small nerve structures[35]. Similar to that, in ultrasound, the CSA calculation also depends on an accurate perpendicular position of the transducer at a certain marker. In neurosonographic measurements of CSA, the inherent variation in the inter-rater variability for ultrasound measurements is a general limitation that also applies to this study.

On the other hand, markings for each level on the surface – which are applied to the skin with a ruler for SSNCS and neurosonography – may differ with respect to the actual anatomical position of the nerve, which in MRN is directly determined by measuring the intervals along the course of the ulnar nerve. This finding should be considered also in a clinical setting, when additional testing is to be performed.

Furthermore, it was shown by Omejec et al. that SSNCS and neurosonography changes at different anatomical positions correlate with the underlying etiology.[7] The authors demonstrated that in individuals with largest CSA and SSNCS latency changes in the range P2 to P0, a nerve compression of the ulnar nerve under the retroepicondylar groove can be assumed, and with greatest CSA and greatest deceleration between P0 and D2, a compression in the region of the humeroulnar aponeurosis can be regarded as causative.[7] Compression of the nerve at the level of the HUA is believed to result from an ongoing transformation of the thin retinaculum of the cubital tunnel into a tough fibrous band, which entraps the nerve. In contrast, compression at the level of the RTC is assumed to be caused by extrinsic compression of the ulnar nerve due to frequent and lasting elbow positioning on a hard surface.[7]

Therefore, separate peaks of measurements in different diagnostic tests in this study might correlate with distinct specificity of a test for a certain etiology. In a further study with more patients and follow-up, correlation with surgical findings is desirable.

In this study as well – even though there were discrepancies between tests with respect to the extent of measurements – the difference between affected arms of patients and healthy control arms were most frequently the largest at measure intervals D2 to P0 and P0 to P2 for electrophysiological testing, or measure points P0 and P2 for all other devices.

At these measure points, diagnostic performance was similar for electrodiagnostical testing for the interval P2 - P0, with CSA in neurosonography, CSA in MRN and FA of DTI in P0/P2. At the interval from D2 to P0, diagnostic performance of electrodiagnostical testing was inferior to other tests. At both levels P0 and at P2, T2 CNR of MRN and MD of DTI-based MRN performed slightly better.

Results in the light of existing literature:

Binary comparisons of the methods of this study are in line with recent literature: Generally, diagnostic performance of electrodiagnostical testing with SSNCS for UNE is reported to be accurate with AUC of 0.85 (95% CI: 0.77 – 0.92) and superior to accuracy of CSA in Neurosonography.[5, 17]For CSA in neurosonography, Omejec et al. reported AUCs of 0.77 (95% CI: 0.68–0.86) for a maximum expression at P0 or P2.[5]

Beekman et al. obtained the largest diameter of the ulnar nerve at any of the equivalent levels from P2, P0, and D2 (AUC = 91, 95% CI: 84 - 95).[11] A recent study by Terayama et al. found a maximum CSA at a corresponding position to P0 and derived an AUC of 0.96 for neurosonography and an AUC of 0.95 for MRN.[36]

For CSA in MRN, Baeumer et al. reported an AUC of 0.95, 95% CI: 0.85 - 1.00 for P0, whereas Breitenseher et al. derived an AUC of 0.815 in the cubital tunnel and measured a mean CSA of 0.26 cm^2 (sd, ±0.087) in patients and a mean CSA of 0.18 cm^2 (sd, ±0.038) in healthy controls.[24, 25]

Prior studies even showed better results for diagnostic performance of T2 CNR: Baeumer et al. obtained results for T2 CNR in MRN, with an AUC of 0.94; 95% CI: 0.87 - 1.00) for P0 and Breitenseher et al. calculated also a very good diagnostic performance with an AUC of 0.92.[24, 25]

Recently, DTI has been proven as clinically feasible for the assessment of ulnar nerve pathology in patients with UNE.[25, 37]

Hereby DTI derives estimates of water diffusion in nerve tissue. The quantitative degree of anisotropy of water diffusion can be described by the FA. Reduced FA values were observed in abnormal conditions with Wallerian degeneration, whereas increased FA values were noted in case of ongoing regeneration. Breitenseher et al. noted a minimum for FA 4 cm distal to the epicondyle corresponding to level of D4 with an AUC of 0.75.[25]

The mean diffusivity (MD) equals the apparent diffusion coefficient (ADC), which is commonly used in MR imaging for the central nervous system (CNS). In the peripheral nerve

system changes in MD were observed in nerve injury associated with fibrosis by Lindberg et. al.[27] For a tractography-based measurement of diagnostic performance of DTI in UNE, Breitenseher et al. published an AUC of 0.86.[25] Breckwoldt et al. demonstrated an AUC of 0.91 95% CI: 0.8 - 1) in neuropathies of arm nerves.[38]

Although DTI is an established technique for the evaluation of nerve integrity in the CNS, its application in the peripheral nervous system is more technically demanding and time-consuming in post-processing. Nevertheless, the peripheral nerves are well suited for DTI given their high directionality along the axons. Therefore, DTI has the potential to become a clinical biomarker for demyelination and fibrotic changes of the peripheral nerve structure in the brachial plexus.[39, 40, 41]

Apart from the already discussed etiologies of nerve compression at the HUA or RTC, further differential diagnoses of UNE can be considered. In this study, the anatomical sequences of MRN (T1 and T2) and neurosonography were systematically analyzed for structural/morphological changes. The results indicate that in seven cases, imaging raised a suspicion of a causal pathology. MRN and neurosonography demonstrated broad similarities in this regard. Due to the possibilities of dynamic testing in neurosonography, dislocations of the ulnar nerve in terms of subluxations or luxation could be better detected with neurosonography. Detection of abnormalities in patients with UNE with peripheral nerve imaging has been stated before. [11, 42] Future studies with more patients are needed to systematically determine the additional value.

Limitations and strengths

As mentioned earlier, the relatively small number of patients is a major limitation. In a larger study over a longer period of time, more information about the frequency of suspected etiologies of UNE could be obtained, which could help to better determine the additional

diagnostic value of neurosonography and MRN. However, due to the complex and time-consuming study design, it was not ethically and economically justifiable to investigate a larger cohort of patients and subjects from the outset. Also, in the statistical analysis, it was not accounted for repeated measurements and for the tests performed with only a consensus reading, an inter-reader reliability could not be assessed. For MRN, it must also be mentioned that the role of the contrasting agent application could not be evaluated, as the local ethics commission refused permission to administer a contrast agent. The enhancement of a contrast agent, however, could be a further diagnostic sign that would be especially helpful in suspected cases with inflammation or other conditions involving injury of the blood-nerve barrier. Nevertheless, this is the first prospective study comparing this selection of different state to the art tests with respect to the possibilities of point-precise detection of the lesion site. Even though the number of patients in this first study is still small, it can be shown that additional diagnostic tests can help in the precise detection of the lesion site and thus point out possibilities for differential diagnosis.

Implication for research

Further systematic research as outlined by the present study design with larger case numbers are needed to determine the correlation of underlying pathology and location of UNE. As DTI in peripheral nerve imaging especially with its derived parameter MD is a promising technique that could be used as a non-invasive biomarker for localization of UNE, further research should focus on MD

Implications for practice

UNE is still diagnosed primarily on the basis of neurologic examination and patient history, and it is regularly confirmed with electrodiagnostical testing. A main objective of further diagnostic work-up in patients with suspected UNE is the precise determination of the site of

lesion.[32] Subsequently, differential diagnostic considerations can be made based on the localization of the lesion. For this MR neurography and neurosonography with recognition of the spatial or topographical patterns of the lesion as well as the detection of anomalies of the surrounding tissue play an important role. Therefore, the combination of different test might reveal important information for further therapeutic management.

Conclusion

This study revealed differences in diagnostic performance of tests concerning a specific location of UNE, with slightly better results for T2 CNR in MRN and MD of DTI-based MRN. In order to localize UNE, the difference between affected arms of patients and healthy control arms were most frequently the largest at measure intervals D2 to P0 and P0 to P2 for electrophysiological testing, or measure points P0 and P2 for all other devices. Additional testing with MRN and neurosonography is recommended to uncover anatomical changes. DTI with its derived parameter MD is a promising technique that could be used as a non-invasive biomarker for localization of UNE.

References:

1. American Association of Electrodiagnostic M, Campbell WW. Guidelines in electrodiagnostic medicine. Practice parameter for electrodiagnostic studies in ulnar neuropathy at the elbow. Muscle Nerve Suppl. 1999;8:S171-205.
2. Azrieli Y, Weimer L, Lovelace R, Gooch C. The utility of segmental nerve conduction studies in ulnar mononeuropathy at the elbow. Muscle Nerve. 2003;27(1):46-50.
3. Visser LH, Beekman R, Franssen H. Short-segment nerve conduction studies in ulnar neuropathy at the elbow. Muscle Nerve. 2005;31(3):331-8.
4. Yuksel G, Karlikaya G, Tutkavul K, Akpinar A, Orken C, Tireli H. Electrodiagnosis of ulnar nerve entrapment at the elbow. Neurosciences (Riyadh). 2009;14(3):249-53.
5. Omejec G, Podnar S. Normative values for short-segment nerve conduction studies and ultrasonography of the ulnar nerve at the elbow. Muscle Nerve. 2015;51(3):370-7.
6. Beekman R, Visser LH, Verhagen WI. Ultrasonography in ulnar neuropathy at the elbow: a critical review. Muscle Nerve. 2011;43(5):627-35.
7. Omejec G, Podnar S. Precise localization of ulnar neuropathy at the elbow. Clin Neurophysiol. 2015;126(12):2390-6.
8. Van Den Berg PJ, Pompe SM, Beekman R, Visser LH. Sonographic incidence of ulnar nerve (sub)luxation and its associated clinical and electrodiagnostic characteristics. Muscle Nerve. 2013;47(6):849-55.
9. Ayromlou H, Tarzamni MK, Daghighi MH, et al. Diagnostic value of ultrasonography and magnetic resonance imaging in ulnar neuropathy at the elbow. ISRN Neurol. 2012;2012:491892.
10. Bayrak AO, Bayrak IK, Turker H, Elmali M, Nural MS. Ultrasonography in patients with ulnar neuropathy at the elbow: comparison of cross-sectional area and swelling ratio with electrophysiological severity. Muscle Nerve. 2010;41(5):661-6.
11. Beekman R, Schoemaker MC, Van Der Plas JP, et al. Diagnostic value of high-resolution sonography in ulnar neuropathy at the elbow. Neurology. 2004;62(5):767-73.
12. Gruber H, Glodny B, Peer S. The validity of ultrasonographic assessment in cubital tunnel syndrome: the value of a cubital-to-humeral nerve area ratio (CHR) combined with morphologic features. Ultrasound Med Biol. 2010;36(3):376-82.
13. Mondelli M, Filippou G, Frediani B, Aretini A. Ultrasonography in ulnar neuropathy at the elbow: relationships to clinical and electrophysiological findings. Neurophysiol Clin. 2008;38(4):217-26.
14. Pompe SM, Beekman R. Which ultrasonographic measure has the upper hand in ulnar neuropathy at the elbow? Clin Neurophysiol. 2013;124(1):190-6.
15. Volpe A, Rossato G, Bottanelli M, et al. Ultrasound evaluation of ulnar neuropathy at the elbow: correlation with electrophysiological studies. Rheumatology (Oxford). 2009;48(9):1098-101.

16. Yoon JS, Walker FO, Cartwright MS. Ultrasonographic swelling ratio in the diagnosis of ulnar neuropathy at the elbow. Muscle Nerve. 2008;38(4):1231-5.
17. Omejec G, Zgur T, Podnar S. Diagnostic accuracy of ultrasonographic and nerve conduction studies in ulnar neuropathy at the elbow. Clin Neurophysiol. 2015;126(9):1797-804.
18. Bendszus M, Wessig C, Solymosi L, Reiners K, Koltzenburg M. MRI of peripheral nerve degeneration and regeneration: correlation with electrophysiology and histology. Exp Neurol. 2004;188(1):171-7.
19. Zhang Z, Song L, Meng Q, et al. Morphological analysis in patients with sciatica: a magnetic resonance imaging study using three-dimensional high-resolution diffusion-weighted magnetic resonance neurography techniques. Spine (Phila Pa 1976). 2009;34(7):E245-50.
20. Pham M, Sommer C, Wessig C, et al. Magnetic resonance neurography for the diagnosis of extrapelvic sciatic endometriosis. Fertil Steril. 2010;94(1):351 e11-4.
21. Du R, Auguste KI, Chin CT, Engstrom JW, Weinstein PR. Magnetic resonance neurography for the evaluation of peripheral nerve, brachial plexus, and nerve root disorders. J Neurosurg. 2010;112(2):362-71.
22. Keen NN, Chin CT, Engstrom JW, Saloner D, Steinbach LS. Diagnosing ulnar neuropathy at the elbow using magnetic resonance neurography. Skeletal Radiol. 2012;41(4):401-7.
23. Husarik DB, Saupe N, Pfirrmann CW, Jost B, Hodler J, Zanetti M. Elbow nerves: MR findings in 60 asymptomatic subjects-normal anatomy, variants, and pitfalls. Radiology. 2009;252(1):148-56.
24. Baumer P, Dombert T, Staub F, et al. Ulnar neuropathy at the elbow: MR neurography--nerve T2 signal increase and caliber. Radiology. 2011;260(1):199-206.
25. Breitenseher JB, Kranz G, Hold A, et al. MR neurography of ulnar nerve entrapment at the cubital tunnel: a diffusion tensor imaging study. Eur Radiol. 2015;25(7):1911-8.
26. MacDonaldCL, DikranianK ,Bayly P, et al. Diffusiontensorimagingreliablyde- tects experimental traumatic axonal injury and indicates approximate time of in- jury. J Neurosci. 2007;27:11869–11876.
27. Lindberg PG, Feydy A, Le Viet D, et al. Diffusion tensor imaging of the median nerve in recurrent carpal tunnel syndrome—initial experience. Eur Radiol. 2013; 23:3115–3123.
28. Florence JM, Pandya S, King WM, et al. Intrarater reliability of manual muscle test (Medical Research Council scale) grades in Duchenne's muscular dystrophy. Phys Ther. 1992;72(2):115-22; discussion 22-6.
29. Beekman R, Wokke JH, Schoemaker MC, Lee ML, Visser LH. Ulnar neuropathy at the elbow: follow-up and prognostic factors determining outcome. Neurology. 2004;63(9):1675-80.
30. Kanakamedala RV, Simons DG, Porter RW, Zucker RS. Ulnar nerve entrapment at the elbow localized by short segment stimulation. Arch Phys Med Rehabil. 1988;69(11):959-63.
31 Keen NN1, Chin CT, Engstrom JW, Saloner D, Steinbach LS. Diagnosing ulnar neuropathy at the elbow using magnetic resonance neurography. Skeletal Radiol. 2012 Apr;41(4):401-7.
32 Pham M, Bäumer T, Bendszus M. Peripheral nerves and plexus: imaging by MR-neurography and high-resolution ultrasound. Curr Opin Neurol. 2014 Aug;27(4):370-9.
33 R Core Team (2017). R: A language and environment for statistical computing. R Foundation for Statistical Computing, Vienna, Austria. URL https://www.R-project.org
34 Podnar S, Omejec G1, Bodor M. Nerve conduction velocity and cross-sectional area in ulnar neuropathy at the elbow. Muscle Nerve. 2017 Dec;56(6):E65-E72.
35 Mulder M, Keuken M, Bazin P: Size and shape matter: The impact of voxel geometry on the identification of small nuclei. PLoS One. 2019; 14(4)

36. Terayama Y, Uchiyama S, Ueda K, et al. Optimal Measurement Level and Ulnar Nerve Cross-Sectional Area Cutoff Threshold for Identifying Ulnar Neuropathy at the Elbow by MRI and Ultrasonography. The Journal of Hand Surgery. 2018;(43)6:529-536.
37 Altun Y, Aygun MS, Cevik MU, Acar A, Varol S, Arıkanoglu A, Onder H, Uzar E. Relation between electrophysiological findings and diffusion weighted magnetic resonance imaging in ulnar neuropathy at the elbow. J Neuroradiol. 2013 Oct;40(4):260-6.
38 Breckwoldt MO, Stock C, Xia A, Heckel A, Bendszus M, Pham M, Heiland S, Bäumer P. Diffusion Tensor Imaging Adds Diagnostic Accuracy in Magnetic Resonance Neurography. Invest Radial. 2015 Aug;50(8):498-504.
39 Pham M, Baeumer T, Bendszus M. Peripheral nerves and plexus: imaging by MR-neurography and high-resolution ultrasound. Curr Opin Neurol. 2014;27: 370–379.
40 Chhabra A, Andreisek G, Soldatos T, et al. MR neurography: past, present, and future. AJR Am J Roentgenol. 2011;197:583–591.
41 Ho MJ, Manoliu A, Kuhn FP, Stieltjes B, Klarhöfer M, Feiweier T, Marcon M, Andreisek G.. Evaluation of Reproducibility of Diffusion Tensor Imaging in the Brachial Plexus at 3.0 T. Invest Radiol. 2017 Aug;52(8):482-487.
42 Schertz M, Mutschler C, Masmejean E, Silvera J. High-resolution ultrasound in etiological evaluation of ulnar neuropathy at the elbow. Eur J Radiol. 2017 Oct;95:111-117.